Nonlinear Theory of Laser Imprint, Richtmyer-Meshkov and Rayleigh-Taylor Instabilities

K. Nishihara 1), M. Muarakami 1), C. Matsuoka 2), N. Ohnishi 1), T. Ikegawa 1), Y. Fukuda 1), A. Sunahara 1), H. Nagatomo 1), H. Takabe 1), K. Mima 1)

1) Institute of Laser Engineering, Osaka University, Osaka, Japan
2) Faculty of Science, Ehime University, Matsuyama, Japan

e-mail contact of main author: nishihara@ile.osaka-u.ac.jp

Implosion process in laser fusion can be divided into three phases: start-up, acceleration and stagnation phases and various hydrodynamic instabilities appear in each phase. Analytical models are developed to study nonlinear evolutions of the hydrodynamic instabilities in these phases, and compared with multi-dimensional simulations. We mainly discuss the formation of double spiral structures caused by the singularity of vorticity in the RM spikes, the effect of the ablative stabilization in nonlinear growth of the RT instability with a finite bandwidth and the effect of the radiation cooling on the stability in the stagnation phase. Various smoothing effect, such as radiation smoothing and hydrodynamic smoothing, are also studied in the start-up phase.

1. Introduction

A laser implosion process can be divided into three phases: start up, acceleration and stagnation phases. In the start-up phase, a shock wave driven by the laser ablation propagates through a shell, and the shell acceleration then follows. Hydrodynamic perturbation growth in the start-up phase seeds perturbations of the Richtmyer-Meshkov (RM) instability and the Rayleigh-Taylor (RT) instability in the subsequent phases. The study of the hydrodynamic perturbation growth, such as imprint, in the start-up phase is thus essential for better understanding of implosion uniformity. Hydrodynamic perturbation growth in the start-up phase was investigated by using an analytical model [1]. The model agreed well with simulations and experiments. Various smoothing effects on laser imprint, such as radiation smoothing and hydrodynamic smoothing, are studied for perturbations with relatively short wavelength with the use of two-dimensional hydrodynamic code in Sec. 2.

Wouchuk and Nishihara [2] presented an analytical model for the linear RM instability, which was applicable for both reflected shock and rarefaction. Their analytic formula of the linear growth rate indicates that the RM instability occurs without the impulsive gravitational acceleration, but is driven by the vorticity left by the shocks at the interface. We here consider an unstable interface as a vortex sheet. Most of previous works [3] consider nonlinear evolution of bubbles. However, the growth of spikes plays an important role in the nonlinear phase, because they grow faster than the bubbles. We present a new analytical model that describes a fully nonlinear evolution of the bubble and spike in the RM instability in Sec. 3.

Initial perturbation generally consists of a finite spectrum width of modes due to target imperfections and irradiation nonuniformity. Haan [4] is the first who pointed out that a group of modes with nearly equal value of wave number creates local amplitude. However he assumed that the root mean square (rms) amplitude of the neighboring modes determined the saturation of the linear growth. We have developed a self-consistent weakly nonlinear theory of the RT instability for initial perturbations with a finite spectrum width, taking the third nonlinearity into account [5]. We show that the onset of linear growth saturation is determined from local maximum amplitude instead of the rms amplitude in Sec. 4. Ablative stabilization effect is also found in the weakly nonlinear stage.

In Sec. 5, we discuss the convective instability driven by radiative cooling in the stagnation phase of the implosion [6].

2. Imprint Mitigation in Foam Buffered Target

We have investigated the mitigation of laser imprint in a foam buffered target [7], low-density foam attached on a plastic target, with the use of two-dimensional hydrodynamic code. For a short wavelength perturbation, the deformation of the ablation surface is found to be limited within a small value, since the large blow-off velocity in the foam leads to the decoupling of the ablation surface from the laser absorption region in early time. The deformation of the ablation surface oscillates after the decoupling and it does not grow. By coating a thin gold layer with 5 nm thickness on the foam we obtain additional reduction of the growth. Figure 1 shows the perturbation growth of areal mass density for three different targets with the wavelength of 20 μm in the laser non-uniformity. The total x-ray emission reaches 30% of the absorbed laser energy. Since the x-ray radiation is absorbed mostly at the vicinity of the ablation surface, the amplitude of the surface deformation is damped. The clear reduction of the perturbation growth is found in the imprint phase in the foam buffered target coated with thin gold.
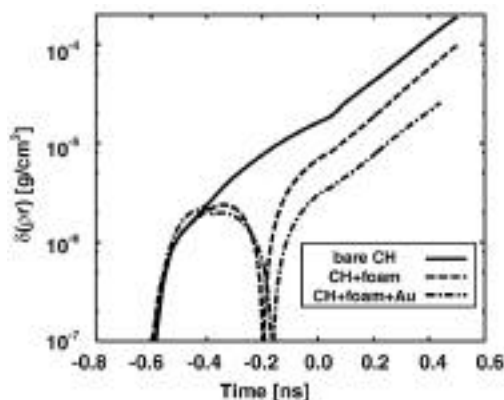

Fig. 1. Growth of areal mass-density perturbation for three different targets, CH, CH+foam (20μm) and CH+foam+Au (5nm). The imprint pulse has 20% spatial non-uniformity of intensity. The imprint pulse of $4x10^{12}W/cm^2$ is irradiated for 600 ps before the main pulse of $7x10^{13}W/cm^2$.

3. Nonlinear Evolution of Richtmyer-Meshkov Instability as Vortex Sheet

In the nonlinear stage of the RM instability, the heavy fluid penetrates into the light fluid and forms spikes. The interface, which separates two different fluids, eventually rolls up like a mushroom as shown in Fig. 2. The transmitted and reflected shocks (or rarefaction) leave the vorticity at the interface. By treating the interface as a vortex sheet with proper boundary conditions, i.e., the continuity of pressure and normal velocity at the interface, we can analytically describe the fully nonlinear dynamics of the interface. Even if we initially consider a pure sinusoidal corrugation of the interface, higher harmonics appears when a shock wave crosses the interface. Thus the vortex sheet is spatially inhomogeneous and the vorticity along the interface contains the higher harmonics. The analytical results show that the second harmonics has generally an opposite sign of the vorticity although its sign and amplitude are determined from the Atwood number and the strength of the incident shock. The opposite sign of the second harmonics was observed in the feed-out experiment [8]. The analytical solutions also indicate that the leading term of the nonlinear growth of the n-th harmonics is proportional to t^n in time and the length of the interface increases proportional to

time. Those properties of the vortex sheet are quantitatively confirmed in two-dimensional simulations.

Figures 2(a) and (b) show the spiral structure of the spike and the vorticity in the nonlinear stage. The spiral structure has been observed in the experiment [9]. The spiral structure of the vortex sheet is analytically obtained by using the Birkhoff-Rott equation with the pressure continuity condition. The dots in the figure are obtained using the surface tracking method. They are initially distributed uniformly along the interface, i.e., with equal distances between the dots. The nonuniform distribution of the dots in the nonlinear stage indicates that the interface is stretched or shrinks locally. The local expansion and contraction of the interface is determined from the sign of the local vorticity along the interface. As shown in Fig. 2(b), the sign of the local vorticity changes along the interface. We can analytically calculate the local vorticity by summing up the higher harmonics of the vorticites. The singularity of the vorticity results in the spiral structure of the spike. The expansion speed of the spiral is proportional to the square of the initial corrugation amplitude.
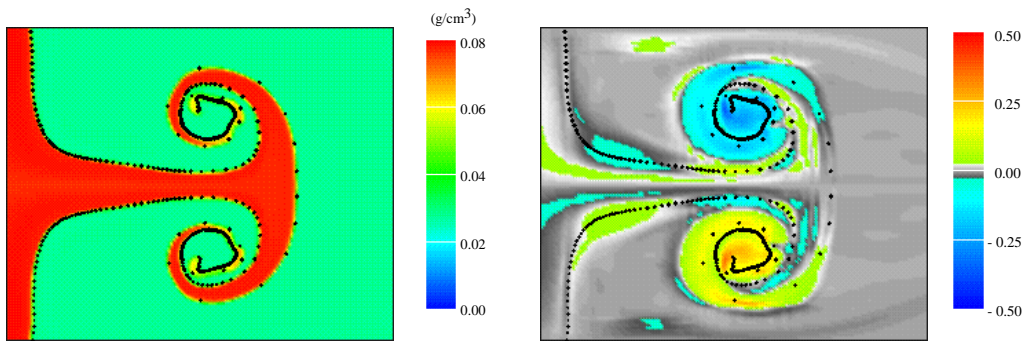

Fig. 2. Spiral structure of spike in nonlinear phase of the RM instability, left and right figures show density and vorticity contours, respectively. Dots present the interface and initially they are distributed uniformly along the interface.

We have also studied the stability of the vortex ring in the RM instability [10] with the use of three-dimensional code IMPACT [11]. Phase rotation of the vortex ring in the azimuthal direction was observed as the expansion of the spike and the roll up of the spiral. However it is relatively stable, i.e., no tilt occurs in a case that there is no split-off of the spike axis.

4. Weakly Nonlinear Evolution of Rayleigh-Taylor Instability with Finite Bandwidth

We consider an initial perturbation of an interface between inviscid, incompressible fluids with a finite bandwidth, $\mathbf{k}= \mathbf{k}_0+ \mathbf{k}$, where $\mathbf{k}$ has discrete allowed values (2 m/L, 2 n/L and L is a system size) for integers m, n, and $|\mathbf{k}_0|>| \mathbf{k}|$. By introducing a complex amplitude of the perturbation varying slowly in space and taking the third order nonlinearity into account, we can derive coupled equations that describe the linear and weakly nonlinear growth of the RT instability. It was shown that the analytical solutions agreed fairly well with two-dimensional simulations including nonlinear phase change of the individual modes [5], that previous works had not resolved.

We have investigated dependence of the saturation amplitudes on the initial spectrum width of modes and initial phase difference among the modes. To clarify that the onset of the linear growth saturation is determined from the local maximum amplitude instead of the rms amplitude, we consider two cases, no phase difference among the modes and random phase. It should be noted that in the case of no phase difference there is only one local peak, but in the

random phase case there are many small local peaks because of the interference among the modes. The results show that the saturation of the linear growth occurs when the local maximum amplitudes reach about $k_0 \xi_{max} \sim 0.15$ for both cases. Even if the maximum of the local peaks saturates, other local peaks continually grow until they reach the saturation amplitude. The saturation amplitude is independent of the initial bandwidth, but weakly depends on the Atwood number. The normalized saturation amplitudes decrease with the increase of the Atwood number. Here we discuss the relation of our results with Haan's model [4]. The rms saturation amplitude is estimated from the square root of the number of states, N_s, as $\xi_{rms}=N_s^{1/2} S(k_0)$. The number of states for the initial spectrum is given by $N_s =(\delta k_0/ \delta k_{min})^2=(k_0 L \delta k_0/k_0 2\pi)^2$. Since the saturation of the linear growth is determined from the local maximum amplitude, we obtain $S(k_0)=(4\pi^2 /k_0^2 L)(\xi_{rms}/ \xi_{max}) \xi \approx (0.3\pi / k_0^2 L)(\xi_{rms}/ \xi_{max})$, where $k_0 \xi_{max}=2 \times 0.15$, $\xi = \delta k_0/k_0$ and $\xi_{rms}/ \xi_{max} \approx 1/3$ for the random phase case. Thus the self-consistent weakly nonlinear theory resolves the assumptions in the Haan's model.

In a weakly nonlinear stage, both local maximum and rms amplitudes grow approximately proportional to time as $k_0 \xi_{max}, k_0 \xi_{rms} \approx 0.2 \gamma_1 t$ for the duration of $\gamma_1 t \leq 2.5$ as shown by thick lines in Fig. 3. In the weakly nonlinear stage the spectrum width increases very rapidly. By taking the ablation effect into account, it is found that the reduction of the weakly nonlinear growth occurs for the short wavelength perturbations of which the second harmonics is stabilized. In this case the weakly nonlinear stage continues for long time up to $\gamma_1 t \approx 13$ due to the smaller nonlinear growth rate as shown in Fig. 3 [5].
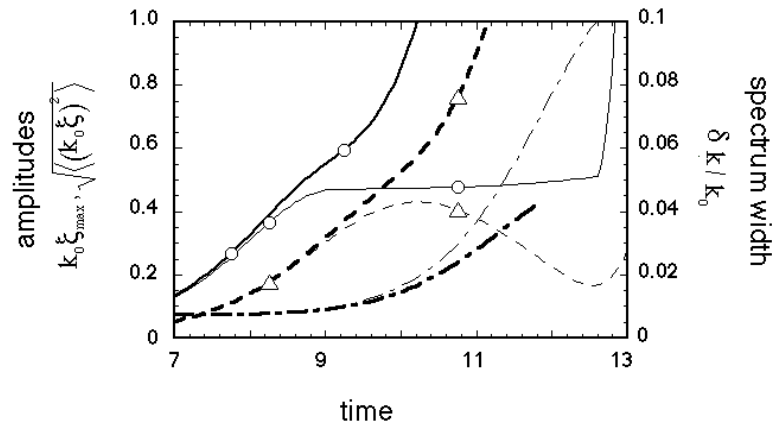

Fig. 3. Temporal evolution of maximum amplitudes (dotted line) and rms amplitudes (solid line) and spectrum width, $\delta k_0/k_0$ (dash-dotted lie), in the case of random phase with initial spectrum width of $\delta k_0/k_0=2\times10^{-3}$ (circles), and 1.6×10^{-2} (triangles). Thin lines indicate the case with the ablation effect.

5. Convective Instability of Radiatively Cooling Self-Similar Implosions

Now, we shed light on the role of radiative cooling, which induces convectively driven instabilities, by means of a new self-similar solution [6,12], where the basic assumption is the power law dependence of the conduction coefficient. The self-similar profiles of the temperature, density, and pressure are all monotonically decreasing functions with radius, and the acceleration is always in the direction of away from the center. In such a system, no RT type instability is anticipated. However, a convective instability is still possible.

To analyze the linear convective instability, we introduce the displacement vector, $\delta\mathbf{r}$, perturbed from its symmetrical self-similar motion with the Lagrangian variable such that $\mathbf{r}(\mathbf{x},t) = \mathbf{r}_0(\mathbf{x},t) + \delta\mathbf{r}(\mathbf{x},t)$ and $\mathbf{r}_0(\mathbf{x},t) = \mathbf{x}R(t)$: $R(t)$ stands for the temporal characteristic scale

length of the considered mass. In the analysis, we assume the perturbation is expressed in the variable separation form: $d\mathbf{r} = \mathbf{H(x)}$ (t). Then these relations are put into the linearization of the equation of motion, which was derived in Ref.[6]. We then introduce the relative amplitude, which is a measure of the effective perturbation growth in a spherically contracting system and is more practical than the absolute amplitude itself, defined by [13] $G(t_1,t) =$ ((t)/R(t))/((t_1)/R(t_1)). As a result we have found that the relative growth shows the conspicuous dependency, i.e., being composed of two parts proportional to t_1 and t_1^2. Physically, this proportionality is easily understood by recalling that the system size reduces with time at an almost constant rate except for the stagnating point. Therefore, if the initial motion of perturbation is set at rest, the perturbation amplitude is kept constant at its initial value, while the system size R(t) reduces with time, and thus the relative amplitude grows according to the reduction of R(t).

Here it should be noted that the linear-in-time perturbation growth can also be observed for a special case with coasting motion, i.e., so-called the Bell-Plesset instability, in which surface waves between two fluids of different densities grow due to the convergent effect. The perturbation growth in the present system, of course, suffers from the convergent effect. Therefore, the linear-in-time dependence is interpreted such that the convergent effect appears in the perturbation growths through the implosion, which are launched when they become convectively unstable.

6. Summary

We have investigated nonlinear evolution of hydrodynamic instabilities in three phases of the laser implosion. The imprint mitigation is shown in a foam buffered target coated with thin gold. Analytical nonlinear theories have been developed for the RM and RT instabilities. Both agree well with multi-dimensional simulations. The nonlinear evolution of the RM instability is described as the self-interaction of a vortex sheet. The onset of the linear growth saturation is determined from the local maximum amplitude. The ablation introduces the reduction of the nonlinear growth. A new convectively driven instability is found in the stagnation phase.

References
[1] Nishihara, K. et al., Phys. Plasmas **5**, 1945 (1998); Ishizaki, R. and Nishihara, K., Phys. Rev. Lett. **78** (1997) 1920; Phys. Rev. E **58** (1998) 3744.
[2] Wouchuk, J. G. and Nishihara, K., Phys. Plasmas **4** (1997) 1028.
[3] Hecht, J. et al., Phys. Fluids **6** (1994) 4019; Alon, U. et al., Phys. Rev. Lett. **74**(1995)534.
[4] Haan, S. W., Phys. Rev. A **39** (1989) 5812.
[5] Nishihara, K. and Ikegawa, T., J. Plasma Fusion Res. SERIES **2** (1999) 536; Ikegawa, T. and Nishihara, K., IFSA99 (Elseiver, edts. Labaune, Hogan, Tanaka, (2000)) 228.
[6] Murakami, M. and Nishihara, K., Phys. Plasmas **7** (2000) 2978.
[7] Nishimura, H. et al., Nucl. Fusion **40** (2000) 547.
[8] Shigemori, K. et al., Phys. Rev. Let. **84** (2000) 5331.
[9] Jacobs, J. W. and Niederhaus, C. E., (to be published).
[10] Fukuda, Y. O. et al., J. Plasma Fusion Res, **75** (1999) 40 (CD-ROM) (in Japanese); IFSA99 (Elseiver, edts. Labaune, C., Hogan, W., Tanaka, K. (2000)) 232.
[11] Sakagami, H. and Nishihara, K., Phys. Rev. Lett., **65** (1990) 432.
[12] Murakami, M., Nucl. Fusion **37** (1997) 549; Basko, M. et al., Phys. Plasmas **5**(1998)518.
[13] Bernstein, I. B. et al., Astrophys. J. **225** (1978) 633.